

# Crystal Structure and Computational Investigation of an Analogue of Grubbs' Second Generation Catalyst with a Fluorous Phosphine

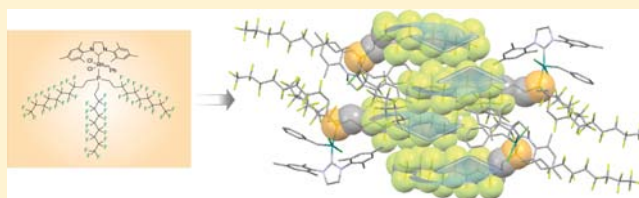
Robert Tuba,<sup>†</sup> Edward N. Brothers,<sup>†</sup> Joseph H. Reibenspies,<sup>‡</sup> Hassan S. Bazzi,<sup>\*,†</sup> and John A. Gladysz<sup>\*,‡</sup>

<sup>†</sup>Department of Chemistry, Texas A&M University at Qatar, P.O. Box 23874, Doha, Qatar

<sup>‡</sup>Department of Chemistry, Texas A&M University, P.O. Box 30012, College Station, Texas 77842-3012, United States

## S Supporting Information

**ABSTRACT:** A fluorous phosphine analogue of Grubbs' second generation olefin metathesis catalyst,  $(\text{H}_2\text{IMes})\text{-}((\text{R}_{18}(\text{CH}_2)_2)_3\text{P})(\text{Cl})_2\text{Ru}(\text{=CHPh})$  (**1**;  $\text{H}_2\text{IMes}/\text{R}_{18} = 1,3$ -dimesityl-4,5-dihydroimidazol-2-ylidene/ $(\text{CF}_2)_7\text{CF}_3$ ) is crystallized and the X-ray structure analyzed in detail. The bond lengths and angles about ruthenium are compared to those of two solvates and five derivatives of Grubbs' second generation catalyst. All exhibit distorted square pyramidal geometries in which the alkylidene ligands occupy apical positions, and geometric trends are interpreted with the help of density functional calculations. The perfluoroalkyl groups (**1**) exhibit helical conformations, as manifested by various torsional relationships, (**2**) segregate in the lattice, and (**3**) align in pairs of opposite helical chiralities.



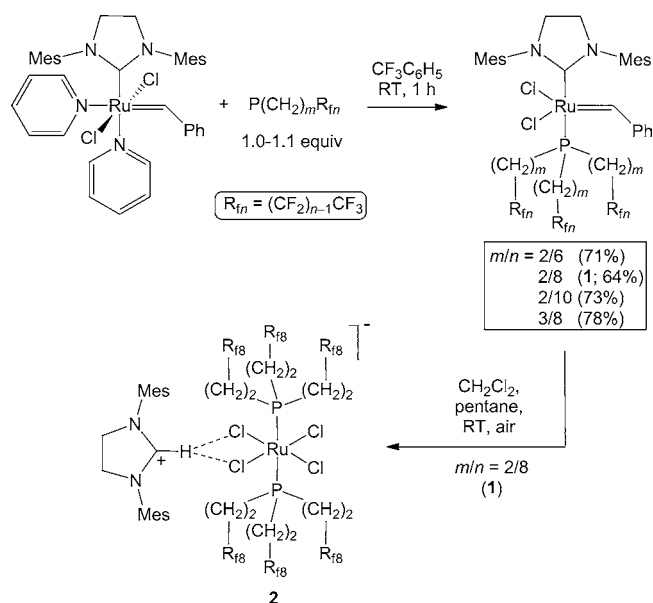
## INTRODUCTION

Both fluorous chemistry<sup>1</sup> and the use of Grubbs' ruthenium catalysts for olefin metathesis<sup>2</sup> have seen exceptional growth over the past two decades. A number of fluorous derivatives of Grubbs' second generation catalyst or the related Grubbs–Hoveyda catalyst have been synthesized.<sup>3,4</sup> In parallel, crystal structures of Grubbs' catalysts<sup>5</sup> and several close relatives<sup>6</sup> have been determined. These have generally been reported as side notes to synthetic studies, with little or no analyses of the geometrical features.

In 1997, there were only two compounds in the Cambridge Structural Database that featured six or more consecutive  $\text{CF}_2$  groups.<sup>7,8</sup> Although this number has grown dramatically,<sup>8–11</sup> crystalline fluorous molecules still remain somewhat of a rarity. In all cases, discrete fluorous domains are found. This can be viewed as a solid state counterpart of the commonly observed spontaneous separations of liquid fluorous and nonfluorous phases.<sup>1</sup> Weakly stabilizing motifs within these fluorous domains have recently been analyzed in detail.<sup>12</sup>

We have prepared analogues of Grubbs' second generation catalyst with a series of fluorous aliphatic phosphines,  $(\text{H}_2\text{IMes})((\text{R}_{18}(\text{CH}_2)_m)_3\text{P})(\text{Cl})_2\text{Ru}(\text{=CHPh})$  ( $\text{H}_2\text{IMes} = 1,3$ -dimesityl-4,5-dihydroimidazol-2-ylidene;  $\text{R}_{18} = (\text{CF}_2)_{n-1}\text{CF}_3$ ) as shown in Scheme 1, and studied their catalytic activity.<sup>4,13,14</sup> In the course of ongoing experiments with the complex with  $m/n = 2/8$  (**1**) that involved a variety of solvents and concentrations,<sup>13</sup> crystals were obtained. These proved amenable to an X-ray crystal structure, the results of which are reported herein. Structural data for related ruthenium complexes are also tabulated, and the trends are interpreted with the help of density functional calculations. The conformations of the fluorinated phosphine substituents and various lattice properties of **1** are analyzed in detail.

## Scheme 1. Syntheses and Aerobic Decomposition of Fluorous Analogues of Grubbs' Second Generation Catalyst



## RESULTS

Crystals of **1** were grown by cooling a toluene solution over an extended period. X-ray data were collected and the structure was determined as summarized in Table 1 and the experimental section. Refinement showed disorder in two of the  $(\text{CH}_2)_2\text{R}_{18}$

Received: July 3, 2012

Published: September 6, 2012

Table 1. Crystallographic Data for **1**

molecular formula	C <sub>38</sub> H <sub>44</sub> Cl <sub>2</sub> F <sub>51</sub> N <sub>2</sub> PRu
molecular mass	1940.89
diffractometer	Bruker D8-GADDS
temperature of collection [K]	110(2)
wavelength [Å]	1.54178
crystal system	monoclinic
space group	P2(1)/n
unit cell dimensions	
a [Å]	13.5824(14)
b [Å]	13.5779(14)
c [Å]	40.186(4)
α [deg]	90
β [deg]	98.797(7)
γ [deg]	90
volume [Å <sup>3</sup> ]	7324.0(13)
Z	4
ρ <sub>calc</sub> [Mg/m <sup>3</sup> ]	1.760
μ [mm <sup>-1</sup> ]	4.197
F(000)	3832
crystal dimensions [mm]	0.13 × 0.06 × 0.01
Θ range [deg]	2.22 to 60.00
range/indeces (h, k, l)	−15,15; −14,15; −45,45
reflections collected	158644
independent reflections	10815 [R(int) = 0.1063]
reflections [I > 2σ(I)]	7056
completeness to Θ = 60.00°	99.4%
max. and min transmission	0.9475 and 0.6135
refinement method	full-matrix least-squares on F <sup>2</sup>
data/restraints/parameters	10815/1905/1525
goodness-of-fit on F <sup>2</sup>	1.005
R indices [I > 2σ(I)]	R <sub>1</sub> = 0.0563, wR <sub>2</sub> = 0.1384
R indices (all data)	R <sub>1</sub> = 0.0819, wR <sub>2</sub> = 0.1460
largest diff. peak/hole [e Å <sup>-3</sup> ]	0.658/−0.661

chains (atoms C12 to C102 and C15 to C105).<sup>15</sup> The dominant conformation of the molecular structure is depicted in Figure 1. The minor chain conformations are not considered in our analyses. Key bond lengths and angles are provided in Table 2 (top). Within the R<sub>48</sub> groups, the average C–C–C and F–C–F angles are 116.6° (σ: 1.0) and 107.3° (σ: 0.9), respectively.

Torsion angles within the (CH<sub>2</sub>)<sub>2</sub>R<sub>48</sub> chains are also presented in Table 2 (middle, bottom). Each four-carbon-atom segment of the nondisordered chain (C11 to C101) exhibited an approximately *anti* conformation, as quantified by torsion angles ranging from 160.3(4)° to 170.9(4)°. The disordered chain running from C12 to C102 was similar, but with a greater range of torsion angles that might reflect artifacts of the disorder (150.8(5)° to 175.6(10)°). In the disordered chain starting at C15, the initial four atom segment exhibited a *gauche* conformation (C15–C25–C35–C45, 53(3)°), but the others were *anti* (158.1(5)° to 167.8(5)°).<sup>16</sup>

Packing diagrams are depicted in Figure 2 and the Supporting Information, Figure S1 (an expanded version of the bottom view in Figure 2). As further elaborated below, the (CH<sub>2</sub>)<sub>2</sub>R<sub>48</sub> chain conformations render **1** chiral, and two molecules of each enantiomer are found in the unit cell (Z = 4), in accord with the achiral space group (P2(1)/n). Other more interpretive aspects of the data are analyzed in the discussion section.

The bond lengths and angles about ruthenium in **1** are compared to those of the methanol and hexafluorobenzene monosolvates of Grubbs' second generation catalyst in Table 3.<sup>5</sup> Data for related complexes with alternative phosphorus donor or alkylidene ligands are also provided.<sup>6</sup> Density functional calculations were conducted as described in the Experimental Section for four representative complexes: **1**, Grubbs' second

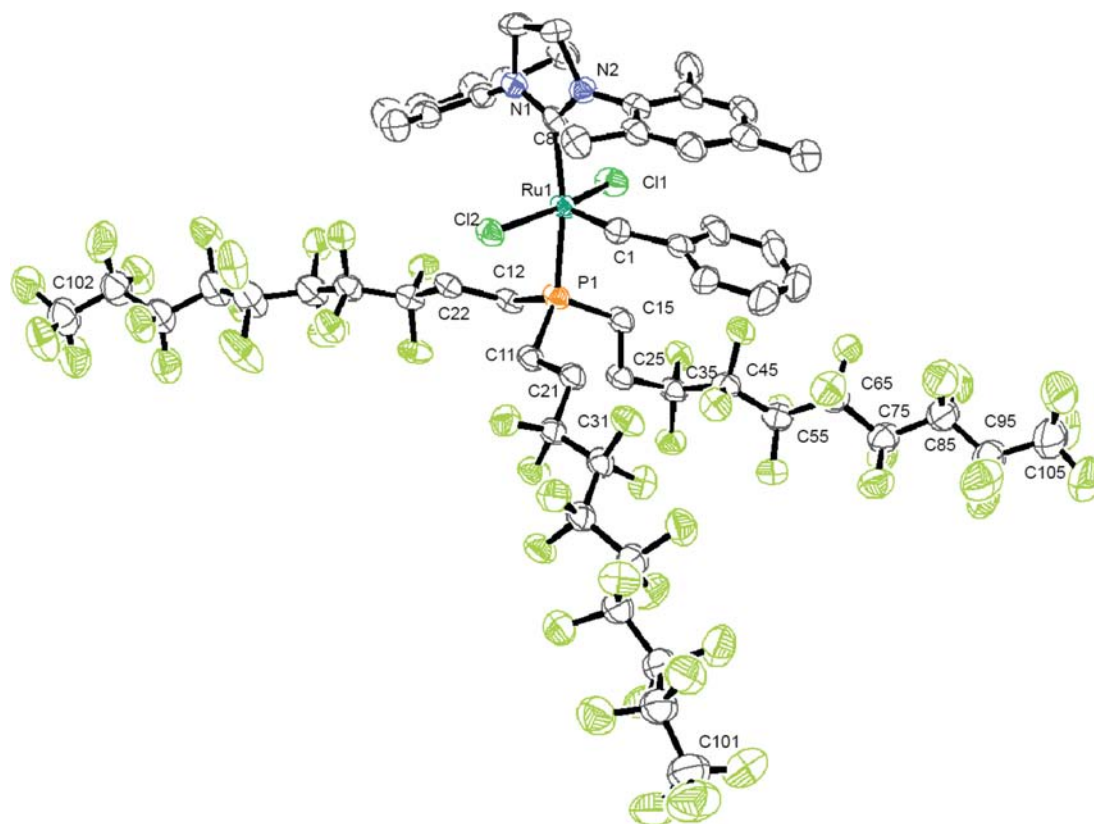


Figure 1. Thermal ellipsoid diagram (50% probability level) of the dominant conformation of the molecular structure of **1**.

Table 2. Key Bond Lengths [Å], Bond Angles [deg], and Torsion Angles [deg] in **1**<sup>a</sup>

Ru1–C1	1.810(5)	Ru1–C8	2.063(5)	Ru1–P1	2.3700(14)
Ru1–Cl1	2.3835(14)	Ru1–Cl2	2.3987(13)	Cl1–Ru1–Cl2	164.70(5)
P1–Ru1–C8	167.20(16)	P1–Ru1–Cl1	84.49(5)	P1–Ru1–Cl2	90.11(5)
P1–Ru1–C1	92.35(16)	Cl1–Ru1–C1	106.98(18)	Cl2–Ru1–C1	87.50(18)
Cl1–Ru1–C8	92.85(14)	Cl2–Ru1–C8	89.26(14)	C1–Ru1–C8	100.4(2)
C11–P1–C12	98.7(7)	C11–P1–C15	105.4(15)	C12–P1–C15	103(2)
Ru1–P1–C11–C21	–66.0(4)	Ru1–P1–C12–C22	–57.9(13)	Ru1–P1–C15–C25	179(3)
P1–C11–C21–C31	–175.5(3)	P1–C12–C22–C32	–171.8(12)	P1–C15–C25–C35	177(3)
C11–C21–C31–C41	164.6(4)	C12–C22–C32–C42	175.6(10)	C15–C25–C35–C45	53(3)
C21–C31–C41–C51	170.9(4)	C22–C32–C42–C52	170.3(8)	C25–C35–C45–C55	158.9(8)
C31–C41–C51–C61	161.0(3)	C32–C42–C52–C62	161.6(6)	C35–C45–C55–C65	162.8(6)
C41–C51–C61–C71	166.1(3)	C42–C52–C62–C72	166.5(6)	C45–C55–C65–C75	162.7(5)
C51–C61–C71–C81	160.3(4)	C52–C62–C72–C82	156.5(6)	C55–C65–C75–C85	167.8(5)
C61–C71–C81–C91	163.9(4)	C62–C72–C82–C92	150.8(5)	C65–C75–C85–C95	158.1(5)
C71–C81–C91–C101	166.5(4)	C72–C82–C92–C102	172.2(6)	C75–C85–C95–C105	167.7(6)
F11–C31–C41–F31	–75.1(4)	F12–C32–C42–F32	171.6(8)	F15–C35–C45–F35	43.7(9)
F11–C31–C41–F41	169.1(3)	F12–C32–C42–F42	55.2(8)	F15–C35–C45–F45	160.0(9)
F21–C31–C41–F31	172.0(3)	F22–C32–C42–F32	–75.1(8)	F25–C35–C45–F35	157.7(8)
F21–C31–C41–F41	56.2(4)	F22–C32–C42–F42	168.6(8)	F25–C35–C45–F45	–86.0(8)
F31–C41–C51–F51	45.3(4)	F32–C42–C52–F52	162.2(7)	F35–C45–C55–F55	–81.8(8)
F31–C41–C51–F61	162.3(3)	F32–C42–C52–F62	44.7(8)	F35–C45–C55–F65	161.0(7)
F41–C41–C51–F51	160.5(3)	F42–C42–C52–F52	–81.6(8)	F45–C45–C55–F55	163.4(7)
F41–C41–C51–F61	–82.5(4)	F42–C42–C52–F62	160.9(7)	F45–C45–C55–F65	46.3(7)
F51–C51–C61–F71	–78.3(4)	F52–C52–C62–F72	167.1(6)	F55–C55–C65–F75	163.5(7)
F51–C51–C61–F81	164.9(3)	F52–C52–C62–F82	51.7(8)	F55–C55–C65–F85	46.5(8)
F61–C51–C61–F71	166.2(4)	F62–C52–C62–F72	–78.2(7)	F65–C55–C65–F75	–80.7(7)
F61–C51–C61–F81	49.5(5)	F62–C52–C62–F82	166.4(7)	F65–C55–C65–F85	162.3(6)
F71–C61–C71–F91	45.6(5)	F72–C62–C72–F92	155.3(7)	F75–C65–C75–F95	52.7(7)
F71–C61–C71–F101	161.8(4)	F72–C62–C72–F102	40.2(8)	F75–C65–C75–F105	168.5(6)
F81–C61–C71–F91	161.1(4)	F82–C62–C72–F92	–89.0(8)	F85–C65–C75–F95	168.6(6)
F81–C61–C71–F101	–82.7(5)	F82–C62–C72–F102	155.9(7)	F85–C65–C75–F105	–75.6(7)
F91–C71–C81–F111	–80.2(5)	F92–C72–C82–F112	36.4(7)	F95–C75–C85–F115	–85.6(7)
F91–C71–C81–F121	163.7(4)	F92–C72–C82–F122	153.1(6)	F95–C75–C85–F125	158.5(6)
F101–C71–C81–F111	163.8(4)	F102–C72–C82–F112	150.4(6)	F105–C75–C85–F115	158.8(6)
F101–C71–C81–F121	47.7(5)	F102–C72–C82–F122	–92.9(7)	F105–C75–C85–F125	42.8(7)
F111–C81–C91–F131	51.5(6)	F112–C82–C92–F132	–72.5(7)	F115–C85–C95–F135	164.5(7)
F111–C81–C91–F141	167.4(4)	F112–C82–C92–F142	170.9(6)	F115–C85–C95–F145	49.4(8)
F121–C81–C91–F131	167.1(4)	F122–C82–C92–F132	171.7(6)	F125–C85–C95–F135	–79.8(8)
F121–C81–C91–F141	–77.0(5)	F122–C82–C92–F142	55.0(8)	F125–C85–C95–F145	165.0(7)
F131–C91–C101–F151	166.3(5)	F132–C92–C102–F152	52.3(8)	F135–C95–C105–F155	55.1(8)
F131–C91–C101–F161	46.5(6)	F132–C92–C102–F162	171.0(7)	F135–C95–C105–F165	174.0(8)
F131–C91–C101–F171	–75.8(6)	F132–C92–C102–F172	–66.5(8)	F135–C95–C105–F175	–62.5(8)
F141–C91–C101–F151	51.6(5)	F142–C92–C102–F152	167.6(7)	F145–C95–C105–F155	168.9(7)
F141–C91–C101–F161	–68.3(6)	F142–C92–C102–F162	–73.6(8)	F145–C95–C105–F165	–72.1(9)
F141–C91–C101–F171	169.5(5)	F142–C92–C102–F172	48.9(8)	F145–C95–C105–F175	51.3(8)

<sup>a</sup>For brevity, the dashes present in the atom labels in the .cif file have been omitted.

generation catalyst, and the P(OEt)<sub>3</sub>/=CHC<sub>6</sub>H<sub>5</sub> and PCy<sub>3</sub>/=CF<sub>2</sub> analogues. These bond lengths and angles are also summarized in Table 3, and the data are interpreted in the following section.

## DISCUSSION

**1. Geometrical Features about Ruthenium.** There have been numerous detailed computational studies of the mechanisms of Grubbs' catalysts, all of which begin with a geometry optimization.<sup>17</sup> However, we are unaware of any experimental or computational analyses of the structural consequences of ligand modification. A critical mass of crystallographic data is

now becoming available, and there are certain to be reactivity ramifications for the many derivatives of Grubbs' second generation catalyst that are now seeing use in metathesis chemistry.

Consider the experimental bond distances in Table 3. Of the five complexes with benzylidene ligands, the Ru=C bond length in **1** (1.810(5) Å) is slightly shorter than in the others (1.836(2)–1.843(4) Å), inclusive of the “three esd” error bar commonly used in crystallographic analyses. Because of the short two-methylene spacer between the phosphorus atom and strongly electron withdrawing R<sub>88</sub> groups, the fluororous phosphine is expected to be the poorest donor ligand in this



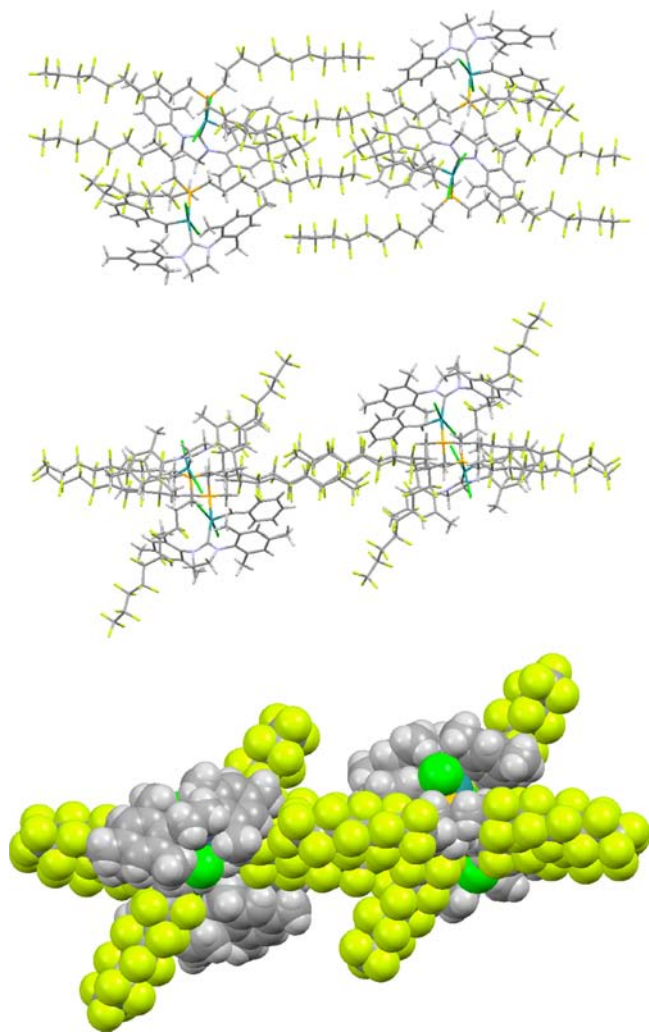


**Figure 2.** Packing diagrams for **1**: top and middle, wire frame representations differing by about a 90° rotation about a horizontal axis in the plane of the paper; bottom, space filling representation of the middle view.

series.<sup>9j,18</sup> Hence, a shorter Ru=C bond is counterintuitive, especially in view of the further contraction in the =CF<sub>2</sub> complex (1.783(2) Å), which features a more accepting ligand.

However, the density functional theory (DFT) computations indicate a longer Ru=C bond in **1** (1.825 Å) than in Grubbs' second generation catalyst (1.819 Å), and a still shorter bond in the =CF<sub>2</sub> complex (1.797 Å). The first distance is 0.015 Å longer than that observed experimentally, whereas the second is 0.017–0.020 Å shorter. Although these deviations are somewhat outside the “three esd” error bar, they represent plausible experimental values. The Ru=C bond length computed for the triethyl phosphite complex (1.827 Å) is comparable to that of **1**, in accord with the weaker donor and stronger π acceptor properties of the phosphorus ligand.<sup>19</sup>

Interestingly, **1** exhibits the shortest Ru–C(H<sub>2</sub>IMes) bond (2.063(5) Å) of all the complexes in Table 3 (2.082(3)–2.125(3) Å). This trend is mirrored computationally (2.068 Å vs 2.075–2.100 Å), and is likely a function of the electronic properties of the opposing phosphorus donor ligand. Both experimentally and computationally, the Ru–P bond in **1** (2.3700(14) or 2.384 Å) is longer than those of the two phosphite complexes (2.3213(10)–2.3496(11) or 2.3431 Å), but shorter than those of the five PCy<sub>3</sub> complexes (2.4268(6)–2.4397(14) or 2.432–2.430 Å). There are no obvious relationships in the Ru–Cl distances.

Consider the experimental bond angles in Table 3. First, the Cl–Ru–Cl and P–Ru–C(H<sub>2</sub>IMes) angles approach 180° (162.8(3)–174.61(5)°), consistent with distorted square pyramidal geometries<sup>5a,6a</sup> in which the benzylidene or alkylidene ligands occupy apical positions. The Cl–Ru–Cl bond angle in **1** (164.70(5)°) is the lowest of all the complexes (174.61(5)–167.27(3)°). This is also paralleled computationally (165.28° vs 165.98–169.44 Å). In contrast, only the two phosphite complexes exhibit P–Ru–C(H<sub>2</sub>IMes) angles greater than **1** (169.23(11)–169.04(9)° vs 167.20(16)° vs 167.08(6)–162.8(3) for the other complexes). An analogous trend is found computationally (168.64° vs 167.34° vs 165.14–164.76°). As judged by the sums of these bond angles, **1** and Grubbs' second

**Table 3.** Experimental and Computed Bond Lengths [Å] and Angles [deg] for Selected Crystallographically Characterized Solvates or Derivatives of Grubbs' Second Generation Catalyst

WebCSD Identifier	GALGOQ <sup>5a</sup>	ICAQEK00 <sup>5b</sup>	QOSMER <sup>6d</sup>	NALTOK01 <sup>6b</sup>	LIBKEN <sup>6c</sup>	ITEHOF <sup>6a</sup>	ITEHIZ <sup>6a</sup>	<b>1</b>	
Ru=C	Exptl.	1.836(2)	1.839(3)	1.838(5)	1.809(11)	1.783(2)	1.843(4)	1.836(4)	1.810(5)
	Calc. <sup>a</sup>	1.819		–	–	1.797	1.827	–	1.825
Ru-C <sup>b</sup>	Exptl.	2.088(2)	2.082(3)	2.087(5)	2.101(10)	2.0872(19)	2.125(3)	2.114(4)	2.063(5)
	Calc. <sup>a</sup>	2.075		–	–	2.082	2.100	–	2.068
Ru-Cl(1) <sup>c</sup>	Exptl.	2.4183(6)	2.391(1)	2.3864(13)	2.396(3)	2.3901(5)	2.3820(10)	2.3605(10)	2.3835(14)
	Calc. <sup>a</sup>	2.437		–	–	2.413	2.415	–	2.426
Ru-Cl(2) <sup>c</sup>	Exptl.	2.3702(6)	2.385(1)	2.3857(14)	2.396(3)	2.3853(5)	2.3985(11)	2.4008(10)	2.3987(13)
	Calc. <sup>a</sup>	2.433		–	–	2.421	2.430	–	2.437
Ru-P	Exptl.	2.4268(6)	2.423(1)	2.4397(14)	2.432(3)	2.4238(5)	2.3213(10)	2.3496(11)	2.3700(14)
	Calc. <sup>a</sup>	2.430		–	–	2.432	2.343	–	2.384
Cl-Ru-Cl	Exptl.	167.66(2)	167.77(3)	174.61(5)	174.05(11)	170.63(2)	167.27(3)	169.23(4)	164.70(5)
	Calc. <sup>a</sup>	167.33		–	–	169.44	165.98	–	165.28
P-Ru-C <sup>b</sup>	Exptl.	164.31(6)	163.91(10)	163.55(14)	162.8(3)	167.08(6)	169.04(9)	169.23(11)	167.20(16)
	Calc. <sup>a</sup>	164.76		–	–	165.14	168.64	–	167.34

<sup>a</sup>See text for the DFT methodology employed. <sup>b</sup>The ligating carbon of the H<sub>2</sub>IMes ligand. <sup>c</sup>When the H<sub>2</sub>IMes ligand is directed up and the alkylidene ligand is oriented to the right, both in the plane of the paper, Cl(1) and Cl(2) are in front and behind the plane of the paper, respectively.

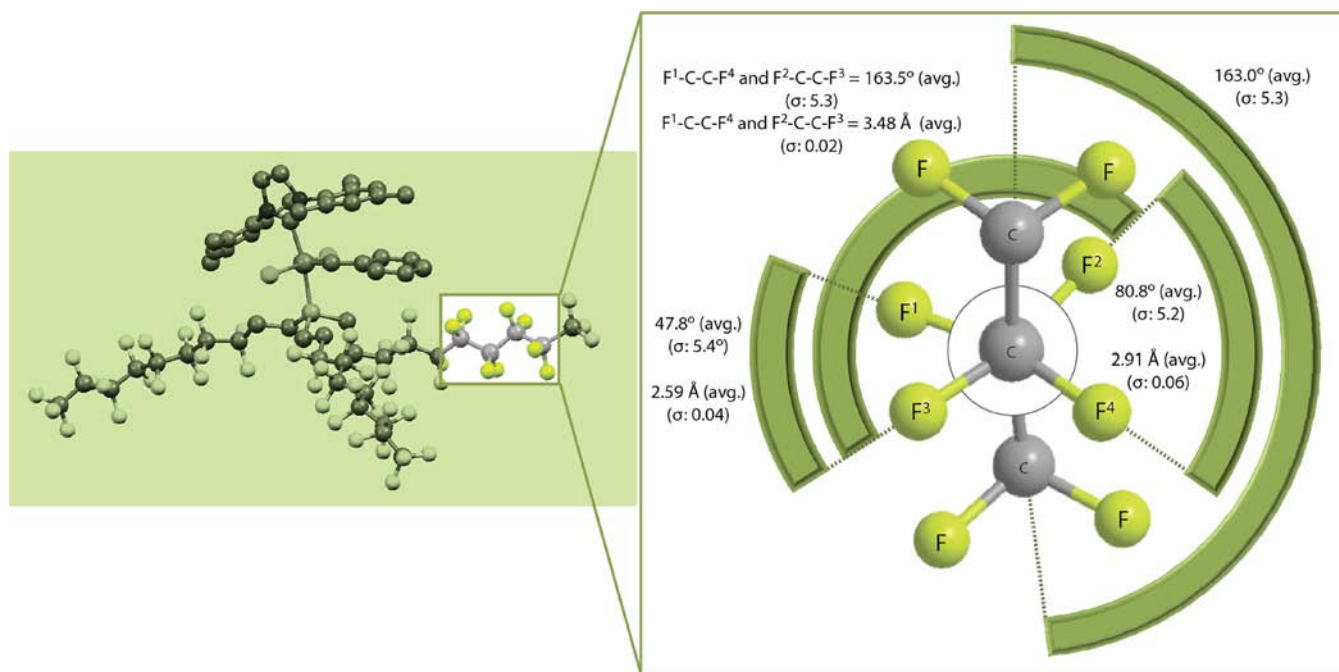


**Figure 3.** Torsional relationships in the perfluoroalkyl groups of **1**.

generation catalyst are the most highly pyramidalized complexes in Table 3.

When one further analyzes the computational data, the bond lengths tend to be systematically overestimated by a small amount (see especially the Ru–Cl and Ru–P values). This is to be expected, as even if one could use a “perfect” functional, the gas phase structures lack the interaction (or “pressure”) generated by neighboring molecules in a crystalline lattice; this interaction would necessarily cause a contraction of the bond lengths. Nonetheless, except for the uncertainties noted with the Ru=C bond lengths, the geometrical parameters and trends therein are well modeled by the functional and basis set employed. Electronic factors obviously play a role, but additional analyses will be required to parse the relative steric and electronic contributions, as well as structural features that may carry reactivity implications.

**2. Conformational and Packing Properties.** Consider properties associated with the  $R_{\text{f8}}$  moieties in **1** next. Many studies have shown that the lowest energy conformations of *n*-perfluoroalkanes and perfluoroalkyl groups exhibit C–C–C–C torsion angles that are somewhat less than those in *n*-alkanes (ca. 180°).<sup>20</sup> The average for the CF<sub>2</sub>–CF<sub>2</sub>–CF<sub>2</sub>–CF<sub>2</sub> linkages in Table 2 is 163.0° (σ: 5.3), as represented schematically in Figure 3. The intrinsic twist in each propagates in the same clockwise or counter-clockwise sense to yield chiral helical poly(difluoromethylene) segments.

One consequence is that the torsion angles between vicinal fluorine atoms in **1** (F–C(C)F–C(C)F–F) generally fall into three regimes, one about 175–160°, one about 85–70°, and one about 50–40°. The last two bookend the value for an idealized gauche conformation (60°). As depicted in Figure 3, the average torsion angles are 163.5° (σ: 5.3), 80.8° (σ: 5.2), and 47.8° (σ: 5.4). There are three corresponding regimes of distances between vicinal fluorine atoms, with averages of 3.48 Å (σ: 0.02), 2.91 Å (σ: 0.06), and 2.59 Å (σ: 0.04), respectively.

The deviation from idealized *anti* conformations in *n*-perfluoroalkanes arises from a complex mixture of factors that includes the

relief of certain electrostatically repulsive interactions, and the generation of new attractive interactions.<sup>21</sup> For example, if the CF<sub>2</sub>–CF<sub>2</sub>–CF<sub>2</sub>–CF<sub>2</sub> torsion angles and C–C–C bond angles are fixed at 180° and 110°, respectively, the gauche vicinal fluorine atoms are separated by only about 2.52 Å,<sup>20a,b</sup> considerably less than the sum of the van der Waals radii (2 × 1.47–1.44 Å or ca. 2.90 Å).<sup>22</sup> However, with decreased torsion angles of 166–167° and increased C–C–C bond angles of 116°, the average gauche fluorine/fluorine separations lengthen to about 2.75 Å.<sup>20a,b</sup> This represents the mean of the average distances (2.59 Å, 2.91 Å) found with **1** (Figure 3).

Within any molecule of **1** in the lattice, the three  $R_{\text{f8}}$  chains exhibit identical helical chiralities. Interestingly, perfluoroalkyl groups can participate in a variety of supramolecular phenomena,<sup>23</sup> including the intertwining of like chiralities to give double helices. VCD measurements have established that helices persist in solution,<sup>24</sup> although naturally the barriers for the interconversion of enantiomers are low.

As shown in Figure 2 and Supporting Information, Figure S1, **1** crystallizes in fluorous and nonfluorous domains. The former is not as dominant or visually dramatic as in complexes with two fluorous phosphines per metal atom. One relevant comparison would be the salt [H<sub>3</sub>IMes]<sup>+</sup> [trans-((R<sub>f8</sub>(CH<sub>2</sub>)<sub>2</sub>)<sub>3</sub>P)<sub>2</sub>Ru(Cl)<sub>4</sub>]<sup>–</sup> (**2**),<sup>10</sup> formed as an oxidation product of **1** as shown in Scheme 1. This gave a high quality, nondisordered structure with more prominent fluorous domains and an average CF<sub>2</sub>–CF<sub>2</sub>–CF<sub>2</sub>–CF<sub>2</sub> torsion angle of 167.2°. In **1**, there are some intramolecular and intermolecular fluorine–fluorine distances that are shorter than the sum of the van der Waals radii,<sup>25</sup> but overall the contacts appeared somewhat “looser” than in other molecules. Given the disorder in two (CH<sub>2</sub>)<sub>2</sub>R<sub>f8</sub> chains, further quantitative analyses were not attempted.

Two of the  $R_{\text{f8}}$  chains in **1** have, because of the flexible intervening (CH<sub>2</sub>)<sub>2</sub>P(CH<sub>2</sub>)<sub>2</sub> moiety, an approximately linear relationship (C102 to C105).<sup>15</sup> Portions of these chains adopt side-by-side relationships with the corresponding segments in other molecules. In these cases, the chains have *opposite* chiralities, an intrinsically less intimate association than with like



chiralities as found in double helices.<sup>23</sup> A portion of the third  $R_{18}$  chain (C31 to C101) similarly pairs with one of opposite chirality from another molecule, as depicted in Supporting Information, Figure S1. An expanded graphic used to assign helical chiralities is provided as Supporting Information, Figure S2.

**3. Conclusion.** In summary, this study has provided useful structural and computational data relevant to (1) Grubbs' second generation catalyst and the growing number of crystallographically characterized derivatives, (2) trends embodied therein, and (3) fluorine molecules with multiple *n*-perfluoroalkyl groups. In accord with observations in earlier studies, the *n*-perfluoroalkyl groups in **1** adopt helical conformations and segregate in the crystal lattice. However, they align in pairs with opposite helical chiralities. Additional properties and applications of **1** will be described in future publications.

## EXPERIMENTAL SECTION

**Computations.** All calculations were performed with the development version of the Gaussian suite of programs,<sup>26</sup> using the  $\omega$ B97XD<sup>27</sup> density functional and the def2-SVP<sup>28</sup> basis set, which was selected as a compromise between accuracy and computational cost. All structures were optimized starting from the crystal structure geometries, and were fully optimized in the gas phase. Gaussian settings were left at their default values except for the integration grid, which was set to "ultrafine", a pruned (99,590) grid.

**Crystallography.** A vial (10 mL) was charged with  $(H_2IMes)-((R_{18}(CH_2)_2)_3P)(Cl)_2Ru(=CHPh)$  (**1**; 10.2 mg, 5.25  $\mu$ mol)<sup>4</sup> and toluene- $d_8$  (3.76 mL) under an argon atmosphere. The pink solution was kept for one month at  $-35^\circ C$ . During this time red plates formed. The supernatant was removed by syringe, and the crystals were dried under oil pump vacuum.

Data were collected as outlined in Table 1.<sup>29</sup> Cell parameters were obtained from 2100 data frames using a  $0.5^\circ$  scan and refined with 6000 reflections. Lorentz and polarization corrections were applied.<sup>29</sup> The program SADABS<sup>30</sup> was employed to correct for absorption effects. The space group was determined from systematic reflection conditions and statistical tests. The structure was solved by SHELXTL (SHELXS).<sup>31</sup> Two of the three  $R_{18}(CH_2)_2$  chains were disordered between two positions. The disorder was modeled by applying a restraint model. Non-hydrogen atoms were refined with anisotropic thermal parameters. The hydrogen atoms were fixed in idealized positions using a riding model. Scattering factors were taken from the literature.<sup>32</sup>

## ASSOCIATED CONTENT

### Supporting Information

A .cif file for **1**, and Figures (S1, S2) illustrating lattice packing. This material is available free of charge via the Internet at <http://pubs.acs.org>.

## AUTHOR INFORMATION

### Corresponding Author

\*E-mail: [gladysz@mail.chem.tamu.edu](mailto:gladysz@mail.chem.tamu.edu) (J.A.G.), [bazzi@tamu.edu](mailto:bazzi@tamu.edu) (H.S.B.).

### Notes

The authors declare no competing financial interest.

## ACKNOWLEDGMENTS

We thank the Qatar National Research Fund for support (NPRP project number 08-607-1-108, experimental work; 09-143-1-022, computational work) and the TAMUQ Research Computing Section of IT for an allocation of computer time.

## REFERENCES

- (a) *Handbook of Fluorous Chemistry*; Gladysz, J. A., Curran, D. P., Horváth, I. T., Eds.; Wiley/VCH: Weinheim, Germany, 2004. (b) *Fluorous Chemistry*; Horváth, I. T., Ed.; Springer: Berlin, Germany, 2012; Topics in Current Chemistry, Vol. 308.
- (2) Vougioukalakis, G. C.; Grubbs, R. H. *Chem. Rev.* **2010**, *110*, 1746–1787.
- (3) (a) Fürstner, A.; Ackermann, L.; Gabor, B.; Goddard, R.; Lehmann, C. W.; Mynott, R.; Stelzer, F.; Thiel, O. R. *Chem.—Eur. J.* **2001**, *7*, 3236–3253. (b) Yao, Q.; Zhang, Y. *J. Am. Chem. Soc.* **2004**, *126*, 74–75. (c) Krause, J. O.; Nuyken, O.; Buchmeiser, M. R. *Chem.—Eur. J.* **2004**, *10*, 2029–2035. (d) Matsugi, M.; Curran, D. P. *J. Org. Chem.* **2005**, *70*, 1636–1642. (e) Michalek, F.; Bannwarth, W. *Helv. Chim. Acta* **2006**, *89*, 1030–1037. (f) Hensle, E. M.; Tobis, J.; Tiller, J. C.; Bannwarth, W. *J. Fluorine Chem.* **2008**, *129*, 968–973. (g) Morton, D.; Leach, S.; Cordier, C.; Warriner, S.; Nelson, A. *Angew. Chem., Int. Ed.* **2009**, *48*, 104–109; *Angew. Chem.* **2009**, *121*, 110–115. (h) Matsugi, M.; Kobayashi, Y.; Suzumura, N.; Tsuchiya, Y.; Shioiri, T. *J. Org. Chem.* **2010**, *75*, 7905–7908.
- (4) (a) Correira da Costa, R. C.; Gladysz, J. A. *Chem. Commun.* **2006**, 2619–2621. (b) Correira da Costa, R.; Gladysz, J. A. *Adv. Synth. Catal.* **2007**, *349*, 243–254.
- (5) Crystal structures of solvates of Grubbs' second generation catalyst and WebCSD identifiers: (a) GALGOQ, Lehman, S. E., Jr.; Wagener, K. B. *Organometallics* **2005**, *24*, 1477–1482. (b) ICAQEK00, Samojłowicz, C.; Bieniek, M.; Pazio, A.; Makal, A.; Woźniak, K.; Poater, A.; Cavallo, L.; Wójcik, J.; Zdanowski, K.; Grela, K. *Chem.—Eur. J.* **2011**, *17*, 12981–12993.
- (6) Crystal structures of analogues of Grubbs' second generation catalyst that feature an alternative phosphorus donor ligand or a =CHCH<sub>3</sub>, =CF<sub>2</sub>, or =CHC≡CAR ligand in place of the benzylidene ligand, and WebCSD identifiers: (a) ITEHOF and ITEHIZ, Schmid, T. E.; Bantreil, X.; Citadelle, C. A.; Slawin, A. M. Z.; Cazin, C. S. J. *Chem. Commun.* **2011**, 47, 7060–7062. (b) NALTOK and NALTOK01 (two structures of an identical compound, 98 and 173 K), Day, M. W.; Trnka, T. M.; Grubbs, R. H. private communication to the CSD and reference Sa. (c) LIBKEN, Macnaughtan, M. L.; Johnson, M. J. A.; Kampf, J. W. *Organometallics* **2007**, *26*, 780–782. (d) QOSMER, Yun, S. Y.; Kim, M.; Lee, D.; Wink, D. J. *J. Am. Chem. Soc.* **2008**, *131*, 24–25.
- (7) (a) Kromm, P.; Bideau, J.-P.; Cotrait, M.; Destrade, C.; Nguyen, H. *Acta Crystallogr.* **1994**, *C50*, 112–115. (b) Jablonski, C. R.; Zhou, Z. *Can. J. Chem.* **1992**, *70*, 2544–2551.
- (8) (a) Guillevic, M.-A.; Arif, A. M.; Horváth, I. T.; Gladysz, J. A. *Angew. Chem., Int. Ed. Engl.* **1997**, *36*, 1612–1615; *Angew. Chem.* **1997**, *109*, 1685–1687. (b) Guillevic, M.-A.; Rocaboy, C.; Arif, A. M.; Horváth, I. T.; Gladysz, J. A. *Organometallics* **1998**, *17*, 707–717.
- (9) Examples involving metal complexes with fluorine alkyolphosphines or phosphites from other research groups: (a) Fawcett, J.; Hope, E. G.; Kemmitt, R. D. W.; Paige, D. R.; Russell, D. R.; Stuart, A. M.; Cole-Hamilton, D. J.; Payne, M. J. *J. Chem. Soc., Chem. Commun.* **1997**, 1127–1128. (b) Haar, C. M.; Huang, J.; Nolan, S. P.; Petersen, J. L. *Organometallics* **1998**, *17*, 5018. (c) Fawcett, J.; Hope, E. G.; Kemmitt, R. D. W.; Paige, D. R.; Russel, D. R.; Stuart, A. M.; Stuart, M. J. *Chem. Soc., Dalton Trans.* **1998**, 3751–3764. (d) Smith, D. C., Jr.; Stevens, E. D.; Nolan, S. P. *Inorg. Chem.* **1999**, *38*, 5277–5281. (e) Stibrany, R. T.; Gorun, S. M. *J. Organomet. Chem.* **1999**, *579*, 217–221. (f) Fawcett, J.; Hope, E. G.; Russel, D. R.; Stuart, A. M.; Wood, D. R. W. *Polyhedron* **2001**, *20*, 321–326. (g) Croxtall, B.; Fawcett, J.; Hope, E. G.; Stuart, A. M. *J. Chem. Soc., Dalton Trans.* **2002**, 491–499. (h) Adams, D. J.; Gudmunsen, D.; Fawcett, J.; Hope, E. G.; Stuart, A. M. *Tetrahedron* **2002**, *58*, 3827–3834. (i) de Wolf, E.; Spek, A. L.; Kuipers, B. W. M.; Philipse, A. P.; Meeldijk, J. D.; Bomans, P. H. H.; Frederik, P. M.; Deelman, B.-J.; van Koten, G. *Tetrahedron* **2002**, *58*, 3911–3922. (j) Malosh, T. J.; Wilson, S. R.; Shapley, J. R. *Inorg. Chim. Acta* **2009**, *362*, 2849–2855. (k) Malosh, T. J.; Wilson, S. R.; Shapley, J. R. *J. Organomet. Chem.* **2009**, *694*, 3331–3337.
- (10) Correira da Costa, R.; Hampel, F.; Gladysz, J. *Polyhedron* **2007**, *26*, 581–588.

- (11) (a) Tuba, R.; Tesevic, V.; Dinh, L. V.; Hampel, F.; Gladysz, J. A. *Dalton Trans.* **2005**, 2275–2283. (b) Consorti, C. S.; Hampel, F.; Gladysz, J. A. *Inorg. Chim. Acta* **2006**, 359, 4874–4884.
- (12) Baker, R. J.; Colavita, P. E.; Murph, D. M.; Platts, J. A.; Wallis, J. D. *J. Phys. Chem. A* **2012**, 116, 1435–1444.
- (13) Tuba, R.; Correa da Costa, R.; Bazzi, H. S.; Gladysz, J. A. *ACS Catalysis* **2012**, 2, 155–162.
- (14) The amount of phosphine specified in the reported synthesis of **1** is incorrect (copy/paste error involving lower homologue).<sup>4b</sup> As with the other complexes in Scheme 1, 1.0–1.1 equiv should be used.
- (15) For brevity, the dashes present in some atom labels in the .cif file are omitted in the text.
- (16) In the minor conformations of the disordered (CH<sub>2</sub>)<sub>2</sub>R<sub>8</sub> chains, the torsional relationships involving the first five carbon atoms are close to those of the major conformations.
- (17) Lead references to an extensive literature: (a) Adlhart, C.; Chen, P. *J. Am. Chem. Soc.* **2004**, 126, 3496–3510. (b) Tsipis, A. C.; Orpen, A. G.; Harvey, J. N. *Dalton Trans.* **2005**, 2849–2858. (c) Sabbagh, I. T.; Kaye, P. T. *J. Mol. Struct.: THEOCHEM* **2006**, 763, 37–42. (d) Zhao, Y.; Truhlar, D. G. *Org. Lett.* **2007**, 9, 1967–1970. (e) Minenkov, Y.; Singstad, Å.; Occhipinti, G.; Jensen, V. R. *Dalton Trans.* **2012**, 41, 5526–5541.
- (18) Jiao, H.; Le Stang, S.; Soós, T.; Meier, R.; Kowski, K.; Rademacher, P.; Jafarpour, L.; Hamard, J.-B.; Nolan, S. P.; Gladysz, J. A. *J. Am. Chem. Soc.* **2002**, 124, 1516–1523.
- (19) Crabtree, R. H. *The Organometallic Chemistry of the Transitions Metals*, 5th ed.; John Wiley & Sons: Hoboken, NJ, 2009; Chapter 4.2.
- (20) (a) Bunn, C. W.; Howells, E. R. *Nature (London)* **1954**, 174, 549–551. (b) Dunitz, J. D.; Gavezzotti, A.; Schweizer, W. B. *Helv. Chim. Acta* **2003**, 86, 4073–4092. (c) Dunitz, J. D. *ChemBioChem* **2004**, 5, 614–621. (d) Kuduva, S. S.; Boese, R. Cambridge Crystallographic Data Centre, Deposition 220154 (2003), refcode OLAWUT.
- (21) (a) Albinsson, B.; Michl, J. *J. Phys. Chem.* **1996**, 100, 3418–3429. (b) Watkins, E. K.; Jorgensen, W. L. *J. Phys. Chem. A* **2001**, 105, 4118–4125. (c) Jang, S. S.; Blanco, M.; Goddard, W. A., III; Caldwell, G.; Ross, R. B. *Macromolecules* **2003**, 36, 5331–5341.
- (22) (a) Bondi, A. *J. Phys. Chem.* **1964**, 68, 441–451. (b) Williams, D. E.; Haupt, D. J. *Acta Crystallogr.* **1986**, B42, 286–295.
- (23) (a) Casnati, A.; Liantonio, R.; Metrangolo, P.; Resnati, G.; Ungaro, R.; Ugozzoli, F. *Angew. Chem., Int. Ed.* **2006**, 45, 1915–1918; *Angew. Chem.* **2006**, 118, 1949–1952. (b) Casnati, A.; Cavallo, G.; Metrangolo, P.; Resnati, G.; Ugozzoli, F.; Ungaro, R. *Chem.—Eur. J.* **2009**, 15, 7903–7912.
- (24) Monde, K.; Miura, N.; Hashimoto, M.; Taniguchi, T.; Inabe, T. *J. Am. Chem. Soc.* **2006**, 128, 6000–6001.
- (25) The shortest intermolecular fluorine-fluorine distance involving the nondisordered (CH<sub>2</sub>)<sub>2</sub>R<sub>8</sub> chain is 2.79 Å (F131–F131, two molecules). Shorter contacts can be found involving the disordered chains.
- (26) Frisch, M. J.; Trucks, G. W.; Schlegel, H. B.; Scuseria, G. E.; Robb, M. A.; Cheeseman, J. R.; Scalmani, G.; Barone, V.; Mennucci, B.; Petersson, G. A.; Nakatsuji, H.; Caricato, M.; Li, X.; Hratchian, H. P.; Izmaylov, A. F.; Bloino, J.; Zheng, G.; Sonnenberg, J. L.; Liang, W.; Hada, M.; Ehara, M.; Toyota, K.; Fukuda, R.; Hasegawa, J.; Ishida, M.; Nakajima, T.; Honda, Y.; Kitao, O.; Nakai, H.; Vreven, T.; Montgomery, J. A. Jr.; Peralta, J. E.; Ogliaro, F.; Bearpark, M.; Heyd, J. J.; Brothers, E.; Kudin, K. N.; Staroverov, V. N.; Keith, T.; Kobayashi, R.; Normand, J.; Raghavachari, K.; Rendell, A.; Burant, J. C.; Iyengar, S. S.; Tomasi, J.; Cossi, M.; Rega, N.; Millam, J. M.; Klene, M.; Knox, J. E.; Cross, J. B.; Bakken, V.; Adamo, C.; Jaramillo, J.; Gomperts, R.; Stratmann, R. E.; Yazyev, O.; Austin, A. J.; Cammi, R.; Pomelli, C.; Ochterski, J. W.; Martin, R. L.; Morokuma, K.; Zakrzewski, V. G.; Voth, G. A.; Salvador, P.; Dannenberg, J. J.; Dapprich, S.; Parandekar, P. V.; Mayhall, N. J.; Daniels, A. D.; Farkas, O.; Foresman, J. B.; Ortiz, J. V.; Cioslowski, J.; Fox, D. J. *Gaussian Development Version*, Revision H.21; Gaussian, Inc.: Wallingford, CT, 2010.
- (27) Chai, J.-D.; Head-Gordon, M. *Phys. Chem. Chem. Phys.* **2008**, 10, 6615–6620.
- (28) Weigend, F.; Furche, R.; Ahlrichs, R. *J. Chem. Phys.* **2003**, 119, 12753–12762.
- (29) GADDS/SAINT; Bruker AXS Inc.: Madison, WI, 2012.
- (30) Sheldrick, G. M. *SADABS, Program for Absorption Correction of Area Detector Frames*; Bruker AXS Inc.: Madison, WI
- (31) Sheldrick, G. M. *Acta Crystallogr.* **2008**, A64, 112–122.
- (32) Fox, A. G.; O’Keefe, M. A.; Tabbarnor, M. A. *Acta Crystallogr.* **1989**, A45, 786–793.